OL Organic Letters

pubs.acs.org/OrgLett Letter

Biomimetic Total Syntheses of Sanctis A−B with Structure Revision

Luqiong Huo, Chunmao Dong, Miaomiao Wang, Xiuxiang Lu, Wenge Zhang, Bao Yang, Yunfei Yuan, Shengxiang Qiu, Hongxin Liu,* and Haibo Tan*

Cite This: https://dx.doi.org/10.1021/acs.orglett.9b04486 Read Online

ACCESS | Metrics & More | Article Recommendations | Supporting Information

ABSTRACT: The first concise total syntheses of sanctis A and B were reported, and it enabled revision of the structure of sanctis B through single-crystal X-ray diffraction. The established synthetic approach mainly mimics a biosynthetic olefin isomerization/hemiacetalization/dehydration/[3 + 3]-type cycloaddition cascade sequence, offering a viable synthetic methodology to efficiently access sanctis A−B and their analogues.

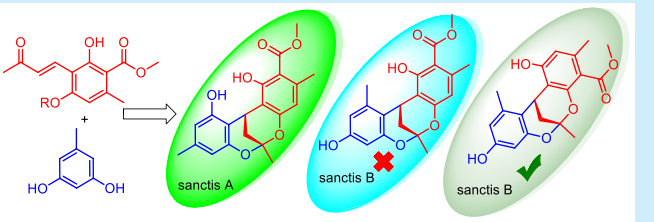

Downloaded via UNIV NOTTINGHAM on January 21, 2020 at 20:09:56 (UTC).
See https://pubs.acs.org/sharingguidelines for options on how to legitimately share published articles.

With the field of phenolic plant metabolites, A-type procyanidins and their analogues are important, because of the prevelance of their represented architectural dioxabicyclo-[3.3.1]nonane scaffold in a wide array of pharmaceuticals and natural products.[1] Especially in "dragon's blood", which is one of the major components of the traditional Chinese hemostatic prescription "Yun-Nan-Bai-Yao", A-type procyanidins have also been verified to exist.[2] Notably, the available data revealed that A-type procyanidins and their analogues are usually endowed with diverse biological properties and potential therapeutic applications, including antioxidant,[1c,3] anti-inflammatory,[4] anti-MRSA,[5] tyrosinase inhibitory,[6] antimicrobial, and antibiofilm activities.[7] Their potent bioactivities and fascinating architectural features have made them appealing targets for synthetic chemists in recent years.[8]

Sanctis A-C are other A-type procyanidin analogues, which were isolated from the Lichen *Parmotrema sancti-angelii* in 2018 (Figure 1).[9] Different from the well-known A-type procyanidin, sanctis A−C (**1**−**3**) feature a unique tetracyclic dioxabicyclo[3.3.1]nonane skeleton with a pendent methyl group, instead of an aromatic ring, displayed at C9. The unprecedented characteristics have driven us to become fascinated with their biological activities, which are significant to gain insight into the structure−activity relationship of A-type procyanidins.[10,11] Nevertheless, the biological activities were rare in the original report, probably because of their poor availability. Attracted by the potential biological activities and their unique structural features, herein, we report the first bioinspired total syntheses of sanctis A−B (**1**−**2**).

With the inspiration of their archtectural characteristics, our hypothetical biogenetic pathway of sanctis A−B (**1**−**2**) was proposed (Scheme 1), which was mainly reflected by their origination from natural product methyl hematommate (**7**)[12] and oricinol **i**[13] with a series of functional group elaboration and dimerization. Briefly, the key biosynthetic precursor **8** might be generated from methyl hematommate **7** via aldol condensation and dehydroxylation. Subsequent olefin isomerization and hemiacetalization reactions can rationally offer hemiacetal **9**. Biosynthetically, hemiacetal **9** may be occupied by orcinol **i** to undergo a remarkable spontaneous hemiacetalization/dehydration/formal [3 + 3] cycloaddition cascade process, similar to our previous strategy utilized in the biomimetic total synthesis of myrtucommuacetalone and myrtucommulone J,[14−16] finishing the construction of unique tetracyclic dioxabicyclo[3.3.1]nonane scaffold. Presumably, both of the target sanctis A−B (**1**−**2**) might be generated simultaneously, depending on the alternative regioselectivity in the process of the formal [3 + 3]-type cycloaddition.

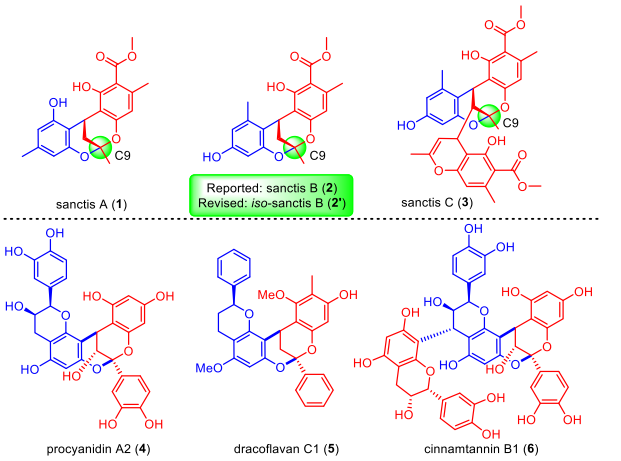

Figure 1. Represent A-type procyanidins and sanctis A−C.

Received: December 14, 2019

© XXXX American Chemical Society

https://dx.doi.org/10.1021/acs.orglett.9b04486
Org. Lett. XXXX, XXX, XXX−XXX

Scheme 1. Proposed Biogenesis of Sanctis A–B

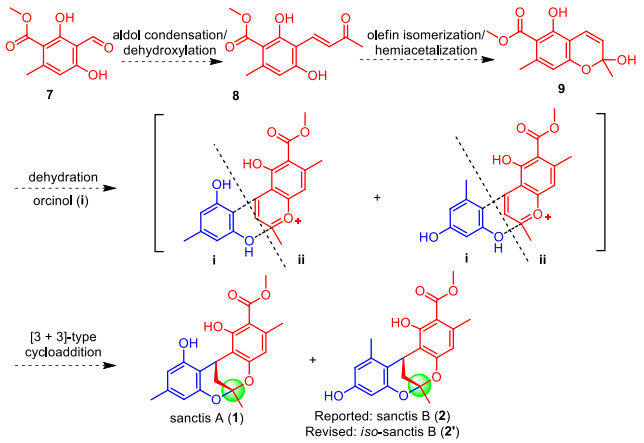

With the scenario in mind, the total syntheses of sanctis A–B (**1**–**2**) mimicking their biogenesis pathway were followed (see Scheme 2). Methyl orsellinate **12** could be obtained

Scheme 2. Biomimetic Total Syntheses of Sanctis A (1) and *iso*-Sanctis B (2′)

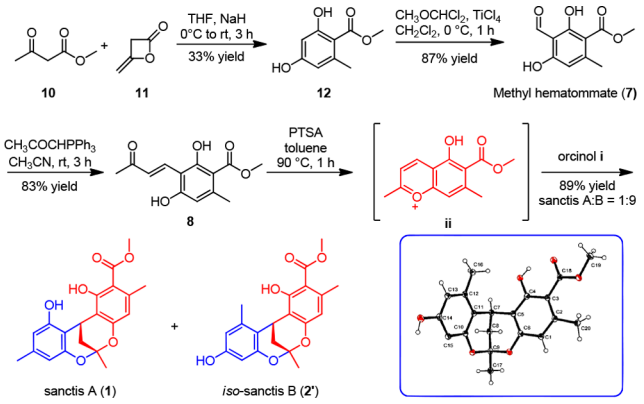

commercially or synthesized from the readily available methyl acetoacetate **10** and lactone **11** in 33% yield.[17,18] The selective formylation of methyl orsellinate **12** then was performed smoothly in the titanium tetrachloride reaction system,[19] resulting in the synthesis of methyl hematommate **7** in 87% yield. **7** could be further converted to biosynthetic precursor **8** using the Wittig reaction with a yield of 83%, as expected. With biosynthetic precursor **8** in hand, the key cascade reaction was conducted with PTSA as a catalyst in toluene at 90 °C. Gratifyingly, the proposed hemiacetalization/dehydration/formal [3 + 3] cycloaddition cascade reaction proceeded smoothly, delivering the desired products sanctis A (**1**) and the putative structure of sanctis B (**2′**) in a combined yield of 89% with a ratio of 1:9, which could be successfully separated via silica gel column chromatography.

Notably, the nuclear magnetic resonance (NMR) and high-resolution electrospray ionization mass spectrometry (HRESIMS) spectra of sanctis A (**1**) fully matched those of the natural isolate. However, the NMR spectra of the synthetic compound **2′**, possessing the putative structure of sanctis B, which was unambiguously established by a single crystal X-ray crystallography, were distinctively inconsistent with those of the natural isolate sanctis B (**2**), as shown in Table 1, although the HRESIMS data showed a very close similarity. The

Table 1. NMR Comparison of Sanctis B and *iso*-Sanctis B

Sanctis B				*iso*-Sanctis B			
No.	**2**	**2′**	$\Delta\delta_H$	No.	**2**	**2′**	$\Delta\delta_C$
H-1	6.32, s	6.28, s	−0.04	C-1	109.9	112.7	−2.8
H-2	–	–	–	C-2	135.9	141.8	+5.9
H-3	–	–	–	C-3	113.0	106.2	−6.8
H-4	–	–	–	C-4	154.4	162.2	+7.8
H-5	–	–	–	C-5	115.7	113.5	−2.2
H-6	–	–	–	C-6	155.3	158.1	+2.8
H-7	4.52, t	4.55, t	+0.03	C-7	24.2	24.1	−0.1
H-8	2.08, m	2.13, m	+0.05	C-8	32.8	32.8	+0.0
H-9	–	–	–	C-9	98.3	98.8	+0.5
H-10	–	–	–	C-10	152.2	154.6	+2.4
H-11	–	–	–	C-11	117.1	117.5	+0.4
H-12	–	–	–	C-12	138.1	138.2	+0.1
H-13	6.23, d	6.26, d	+0.03	C-13	111.3	111.6	+0.3
H-14	–			C-14	157.2	157.5	+0.3
H-15	6.15, brd	6.15, d	+0.00	C-15	101.7	101.9	+0.2
H-16	2.50, s	2.53, s	+0.03	C-16	19.9	20.1	+0.2
H-17	1.72, s	1.77, s	+0.05	C-17	27.3	27.5	+0.2
H-18	–			C-18	168.7	173.7	+5.0
H-19	3.79, s	3.93, s	+0.14	C-19	51.7	52.7	+1.0
H-20	2.10, s	2.43, s	+0.33	C-20	19.4	24.3	+4.9
4-OH	8.94, s	12.08, s	+4.14				
14-OH	8.03, s	8.04, s	+0.01				

informative results collectively pointed to the possibility of incorrect structural establishment for sanctis B (**2**), via the misinterpretation of NMR spectra attributable to its architectural complexity. Moreover, the structure of synthetic product **2′** could be further confirmed by the two-dimensional (2D) NMR interpretation (see Scheme 3), thus strengthening the

Scheme 3. HMBC Correlations of 2 and 2′

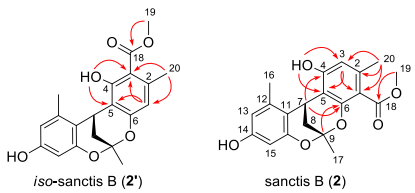

aforementioned conclusion. Based on the aforementioned results, we tentatively concluded that the structure of natural product sanctis B (**2**) was wrongly elucidated and, accordingly, gave the synthetic compound **2′** with a trivial name of *iso*-sanctis B.

In order to further reassign the structure of sanctis B (**2**), a concerted effort to compare the ^{1}H and ^{13}C NMR data between sanctis B (**2**) and *iso*-sanctis B (**2′**) were conducted, and it was readily found that sanctis B (**2**) should exist as a similar isomer also possessing a dioxabicyclo[3.3.1]nonane

https://dx.doi.org/10.1021/acs.orglett.9b04486
Org. Lett. XXXX, XXX, XXX–XXX

Table 2. Optimization of Reaction Conditions[a]

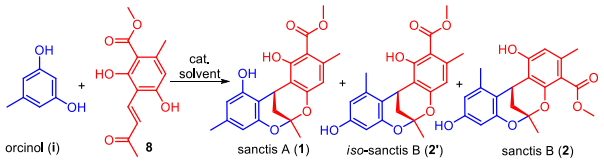

entry	solvent	catalyst	catalyst loading	temperature, T (°C)	time	yield[b] (%)	ratio of 1:2′:2[c]
1	toluene	PTSA	1.0 equiv	rt	4 d	70	1:9:0
2	toluene	PTSA	1.0 equiv	90	1 h	89	1:9:0
3	toluene	PPTS	1.0 equiv	120	3 h	30	0:1:0
4	toluene	TFA	50 μL	90	3 h	30	0:1:0
5	toluene + dioxane[d]	PTSA	1.0 equiv	90	3 h	<10	–
6	toluene + THF[e]	PTSA	1.0 equiv	90	3 h	<10	–
7	THF	PTSA	1.0 equiv	rt	3 h	nr[f]	–
8	DCM	PTSA	1.0 equiv	rt	3 h	50	0:1:0
9	2N HCl + ACN[g]			90	1 h	70	0:1:0

[a]Reaction conditions: **i** (1.2 mmol), **8** (1.0 mmol), solvent (5 mL), rt, 1−3 h. [b]Isolated yield. [c]The ratio was accorded by ^{1}H NMR. [d]Toluene (4 mL), dioxane (1 mL). [e]Toluene (4 mL), THF (1 mL). [f]No reaction. [g]ACN (2.5 mL), 2N HCl (2.5 mL).

scaffold, because of their closely similar NMR profiles. However, the absence of the proton signal at δ_H 12.08 suggested that the phenolic OH in sanctis B (**2**) was not involved in the 1,3-hydrogen bonding effect. Further elucidation of the HMBC spectrum of **2** disclosed that it necessitated to be a regioisomer of *iso*-sanctis B (**2′**). This conclusion could be unambiguously confirmed by the critical HMBC correlations of H_3-20 to C-1, C-2, and C-3, H-3 to C-5 and C-6, in conjunction with 4-OH to C-3, C-4, and C-5. Thus, the reported structure of sanctis B was corrected and depicted as compound **2** in Scheme 3.

The major difference between the structures of sanctis B (**2**) and *iso*-sanctis B (**2′**) was attributed to the alternative selectivity for the two phenolic groups of intermediate **8** participating in the cyclization process (see Table 2). Therefore, the endeavors with the objective to diversely access sanctis A−B (**1**−**2**) as well as *iso*-sanctis B (**2′**) in one operation were performed, and several contributing variables, such as solvents, substrate loadings, and potential acid catalysts, were screened. As a result, the reproducibility of this reaction necessitated strong acids and nonpolar organic solvents, but were accompanied by the reduction of yields (see Table 2, entries 1−8). Moreover, all of them just afforded the products sanctis A (**1**) and/or *iso*-sanctis B (**2′**) with a ratio of ∼1:9 (see Table 2, entries 1 and 2). Especially, the usage of PTSA as the acidic catalyst and toluene as the solvent gives rise to the best yield (89%). Notably, when an aqueous condition was used to mimic the biosynthetic environment in a natural organism, the hemiacetalization/dehydration/formal [3+ 3] cycloaddition cascade sequence proceeded smoothly to generate the target products sanctis A (**1**) and *iso*-sanctis B (**2′**) with 70% yield, strongly suggesting the possibility for the process to be a biomimetic transformation mimicking the natural generation of sanctis A (**1**) and its derivatives downstream, although the use of stronger acid and the absence of sanctis B (**2**) should be further investigated.

Considering the absence of sanctis B (**2**) in the cascade reaction process, we speculated that the priority to generate *iso*-sanctis B (**2′**) instead of sanctis B (**2**) was most probably attributed to the superior reactivity for the *para*-phenolic free hydroxyl functionality than that of the *ortho*-phenolic one in **8** under the nonenzymatic conditions. To probe the mechanism and achieve the biomimetic total synthesis of sanctis B (**2**) with its further structural confirmation, the concise synthetic process with protection for the *para*-phenolic free hydroxyl group of **8** was performed as shown in Scheme 4.

Scheme 4. Biomimetic Total Syntheses of Sanctis B (2)

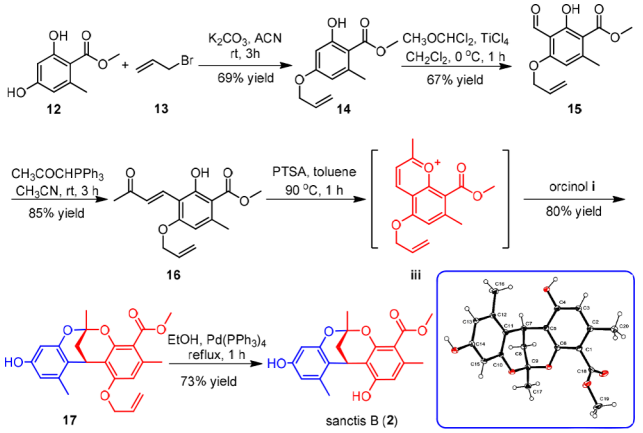

The selective *O*-allylation of the *para*-phenolic free hydroxyl group of phenol **12** with allylic bromide **13** could successfully afford the desired ether intermediate **14** in 69% yield, and further $TiCl_4$-mediated formylation would transform it to the aldehyde **15** in 67% yield. The critical *α*,*β*-unsaturated ketone moiety was readily constructed using the classical Wittig reaction, offering the key precursor **16** in 85% yield, which then underwent the key hemiacetalization/dehydration/formal [3 + 3] cycloaddition cascade reaction with orcinol **i** to efficiently finish the establishment of tetracyclic dioxabicyclo[3.3.1]-nonane scaffold, generating the expected product **17** through the active chromenylium intermediate **iii** in a highly efficient manner. Finally, the deprotection of the allylic group would successfully afford the target product sanctis B (**2**) in 73% yield. To our delight, the NMR and HRESIMS spectra of synthetic product perfectly matched with those of the natural isolate sanctis B (**2**). Moreover, the X-ray diffraction (XRD) analysis experiment was also conducted for the readily crystallized synthetic sanctis B (**2**), thus unambiguously confirming its revised structure. Therefore, we successfully

https://dx.doi.org/10.1021/acs.orglett.9b04486
Org. Lett. XXXX, XXX, XXX−XXX

complete the first biomimetic total synthesis of sanctis B (**2**) and distinctively revised its structure via XRD analysis.

In order to further address the problematic issue on the absence of sanctis B (**2**) during the synthetic cascade process, subsequently, the intertransformation between sanctis B (**2**) and *iso*-sanctis B (**2′**) through the enol ether intermediate **18** was also investigated (see Scheme 5). Treatment of sanctis B

Scheme 5. Intertransformation of 2 and 2′

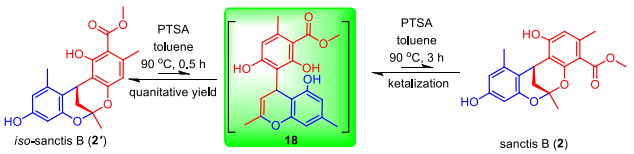

(**2**) with the standard reaction conditions performed in the biomimetic cascade process resulted in complete conversion of **2** to target product **2′** within 0.5 h and at ∼100% yield. However, when **2′** was subjected to the same reaction conditions, none of any desired product **2** was detected, even after 3 h. The aforementioned results collectively highlighted that the **2′** should be a thermodynamically favorable product in an interchange equilibrium, mainly because of its less steric hindrance and the formation of a 1,3-hydrogen bonding effect, logically indicating that **2′** might be generated in part from **2**, because of the presence of a strong acid in our established reaction conditions. Moreover, these results also tentatively answered the issue of why sanctis B (**2**) was discovered in nature but *iso*-sanctis B (**2′**) was only accessed in our biomimetic total synthesis process.

In conclusion, the chemological evolution of the structural entities encoded by nature's molecular archive stimulated us to complete the biomimetic total syntheses of sanctis A−B (**1**−**2**) and *iso*-sanctis (**2′**), in conjunction with unequivocal structure revision of sanctis B (**2**) through XRD. Our synthetic methodology was mainly ascribed to mimic the biosynthetic olefin isomerization/hemiacetalization/dehydration/[3 + 3] cycloaddition sequence, which held the promise of illustrating the possibility of biogenetic pathways for these natural products. Taking the advantage of simplicity and efficiency, we believe that the described synthetic strategy and technologies would provide a general process for the rapid assembly of other such dimer products. Moreover, this study would open new pathways to provide sufficient quantities of these molecules toward the drug discovery in a practical fashion. Further investigations directed toward this goal are currently underway and will be reported in due course.

■ ASSOCIATED CONTENT

Supporting Information

The Supporting Information is available free of charge at https://pubs.acs.org/doi/10.1021/acs.orglett.9b04486.

Experimental section, detailed experimental procedures and full spectroscopic data for all related compounds (PDF)

Accession Codes

CCDC 1970760 and 1970762 contain the supplementary crystallographic data for this paper. These data can be obtained free of charge via www.ccdc.cam.ac.uk/data_request/cif, or by emailing data_request@ccdc.cam.ac.uk, or by contacting The Cambridge Crystallographic Data Centre, 12 Union Road, Cambridge CB2 1EZ, UK; fax: +44 1223 336033.

■ AUTHOR INFORMATION

Corresponding Authors

Hongxin Liu − *Guangdong Institute of Microbiology, Guangdong Academy of Sciences, Guangzhou, China*; Email: liuhx@gdim.cn

Haibo Tan − *South China Botanical Garden, Chinese Academy of Sciences, Guangzhou, China*; orcid.org/0000-0002-1652-5544; Email: tanhaibo@scbg.ac.cn

Other Authors

Luqiong Huo − *South China Botanical Garden, Chinese Academy of Sciences, Guangzhou, China, Guangdong Institute of Microbiology, Guangdong Academy of Sciences, Guangzhou, China, and University of Chinese Academy of Sciences, Beijing, People's Republic of China*

Chunmao Dong − *South China Botanical Garden, Chinese Academy of Sciences, Guangzhou, China*

Miaomiao Wang − *South China Botanical Garden, Chinese Academy of Sciences, Guangzhou, China, and University of Chinese Academy of Sciences, Beijing, People's Republic of China*

Xiuxiang Lu − *South China Botanical Garden, Chinese Academy of Sciences, Guangzhou, China, and University of Chinese Academy of Sciences, Beijing, People's Republic of China*

Wenge Zhang − *South China Botanical Garden, Chinese Academy of Sciences, Guangzhou, China, and University of Chinese Academy of Sciences, Beijing, People's Republic of China*

Bao Yang − *South China Botanical Garden, Chinese Academy of Sciences, Guangzhou, China*; orcid.org/0000-0002-5483-7960

Yunfei Yuan − *South China Botanical Garden, Chinese Academy of Sciences, Guangzhou, China*

Shengxiang Qiu − *South China Botanical Garden, Chinese Academy of Sciences, Guangzhou, China*

Complete contact information is available at: https://pubs.acs.org/10.1021/acs.orglett.9b04486

Notes

The authors declare no competing financial interest.

■ ACKNOWLEDGMENTS

We thank the National Natural Science Foundation of China (No. 81773602), Natural Science Foundation of Guangdong Province (No. 2019A1515011694), Pearl River Science and Technology New Star Fund of Guangzhou (No. 201605120849569), Guangdong Special Support Program (No. 2017TQ04R599), and the Foundation of Key Laboratory of Plant Resources Conservation and Sustainable Utilization, South China Botanical Garden, Chinese Academy of Sciences.

■ REFERENCES

(1) For selected reviews, see: (a) Foo, L. Y.; Lu, Y.; Howell, A. B.; Vorsa, N. *Phytochemistry* **2000**, *54*, 173. (b) Liu, L.; Xie, B.; Cao, S.; Yang, E.; Xu, X.; Guo, S. *Food Chem.* **2007**, *105*, 1446.

(c) Appeldoorn, M. M.; Sanders, M.; Vincken, J. P.; Cheynier, V.; Le Guernevé, C.; Hollman, P. C. H.; Gruppen, H. *Food Chem.* **2009**, *117*, 713. (d) Appeldoorn, M. M.; Vincken, J.-P.; Sanders, M.; Hollman, P. C. H.; Gruppen, H. *J. Agric. Food Chem.* **2009**, *57*, 6007. (e) Kim, I.-S.; Park, Y.-J.; Yoon, S.-J.; Lee, H.-B. *Int. Immunopharmacol.* **2010**, *10*, 1616. (f) Lin, H.-C.; Lee, S.-S. *J. Nat. Prod.* **2010**, *73*, 1375. (g) Li, S.; Xiao, J.; Chen, L.; Hu, C.; Chen, P.; Xie, B.; Sun, Z. *Food Chem.* **2012**, *135*, 31.

(2) (a) Arnone, A.; Nasini, G.; Merlini, L. *J. Chem. Soc., Perkin Trans. 1* **1990**, 2637. (b) Arnone, A.; Nasini, G.; Vajna de Pava, O.; Merlini, L. *J. Nat. Prod.* **1997**, *60*, 971. (c) Toh, Z. S.; Wang, H.; Yip, Y. M.; Lu, Y.; Lim, B. J. A.; Zhang, D.; Huang, D. *Bioorg. Med. Chem.* **2015**, *23*, 7641.

(3) Maldonado, P. D.; Rivero-Cruz, I.; Mata, R.; Pedraza-Chaverri, J. *J. Agric. Food Chem.* **2005**, *53*, 1996.

(4) Lin, L. C.; Kuo, Y. C.; Chou, C. J. *J. Nat. Prod.* **2002**, *65*, 505.

(5) Sasaki, H.; Kashiwada, Y.; Shibata, H.; Takaishi, Y. *Phytochemistry* **2012**, *82*, 136.

(6) Zheng, Z. P.; Cheng, K. W.; To, J. T.; Li, H.; Wang, M. *Mol. Nutr. Food Res.* **2008**, *52*, 1530.

(7) Alejo-Armijo, A.; Glibota, N.; Frías, M. P.; Altarejos, J.; Gálvez, A.; Salido, S.; Ortega-Morente, E. *J. Agric. Food Chem.* **2018**, *66*, 2151.

(8) For selected papers in recent years, see: (a) Ito, Y.; Ohmori, K.; Suzuki, K. *Angew. Chem., Int. Ed.* **2014**, *53*, 10129. (b) Sharma, P. K.; Romanczyk, L. J., Jr; Kondaveti, L.; Reddy, B.; Arumugasamy, J.; Lombardy, R.; Gou, Y.; Schroeter, H. *Org. Lett.* **2015**, *17*, 2306. (c) Schmid, M.; Trauner, D. *Angew. Chem., Int. Ed.* **2017**, *56*, 12332. (d) Guo, Z.; Wang, Z.; Tang, Y. *Org. Lett.* **2018**, *20*, 1819.

(9) Duong, T. H.; Ha, X. P.; Chavasiri, W.; Beniddir, M. A.; Genta-Jouve, G.; Boustie, J.; Chollet-Krugler, M.; Ferron, S.; Nguyen, H. H.; Yamin, B. M.; Huynh, B. L. C.; Le Pogam, P.; Nguyen, K. P. P. *Eur. J. Org. Chem.* **2018**, *2018*, 2247.

(10) Dudek, M. K.; Gliński, V. B.; Davey, M. H.; Sliva, D.; Kaźmierski, S.; Gliński, J. A. *J. Nat. Prod.* **2017**, *80*, 415.

(11) Chen, L.; Yang, Y.; Yuan, P.; Yang, Y.; Chen, K.; Jia, Q.; Li, Y. *Evid. Based Complement. Alternat. Med.* **2014**, *2014*, 365258.

(12) Carpentier, C.; Queiroz, E. F.; Marcourt, L.; Wolfender, J. L.; Azelmat, J.; Grenier, D.; Boudreau, S.; Voyer, N. *J. Nat. Prod.* **2017**, *80*, 210.

(13) Wu, X.; Chen, Z.; Ding, W.; Liu, Y.; Ma, Z. *Nat. Prod. Res.* **2018**, *32*, 1562.

(14) Liu, H. X.; Huo, L. Q.; Yang, B.; Yuan, Y. F.; Zhang, W. M.; Xu, Z. F.; Qiu, S. X.; Tan, H. B. *Org. Lett.* **2017**, *19*, 4786.

(15) Tan, H. B.; Liu, H. X.; Chen, X. Z.; Yuan, Y. F.; Chen, K.; Qiu, S. X. *Org. Lett.* **2015**, *17*, 4050.

(16) Liu, H. X.; Wang, Y.; Guo, X. Y.; Huo, L. Q.; Xu, Z. F.; Zhang, W. M.; Qiu, S. X.; Yang, B.; Tan, H. B. *Org. Lett.* **2018**, *20*, 546.

(17) Ji, X.-Y.; Xue, S.-T.; Zheng, G-H.; Han, Y.-X.; Liu, Z.-Y.; Jiang, J.-D.; Li, Z.-R. *Acta Pharm. Sin. B* **2011**, *1*, 93.

(18) Methyl orsellinate **12** could be also prepared in 65% yield, according to the alternative literature. See: Chiarello, J.; Joullie, M. M. *Tetrahedron* **1988**, *44*, 41.

(19) Grayfer, T. D.; Grellier, P.; Mouray, E.; Dodd, R. H.; Dubois, J.; Cariou, K. *Org. Lett.* **2016**, *18*, 708.

https://dx.doi.org/10.1021/acs.orglett.9b04486
Org. Lett. XXXX, XXX, XXX−XXX